Original Paper

Indoor and Built Environment

Indoor and Built Environment
0(0) 1–12

DOI: 10.1177/1420326X17704276
journals.sagepub.com/home/ibe

SAGE

An analysis of operating parameters in the cooling tower-based thermally activated building system

D. G. Leo Samuel[1], S. M. Shiva Nagendra[2] and M. P. Maiya[1]

Abstract

Thermally activated building system is not only energy efficient but also provides better thermal comfort compared to the conventional cooling systems. In this paper, COMSOL Multiphysics, a computational fluid dynamics tool, is used to simulate the performance of a cooling tower coupled with thermally activated building system for the hot and dry summer climatic conditions of New Delhi. The effects of three operating parameters, namely, temperature and inlet velocity of water and the number of cooling surfaces (area), on the performance of the system have been investigated. The results indicate that increasing the water inlet temperature from wet bulb temperature (WBT) to WBT + 6°C would increase the operative temperature of the indoor space, a thermal comfort index, by 2°C. The increase in water inlet velocity from 0.2 to 1 m/s would decrease the diurnal average of operative temperature by 1.4°C. If only the roof was cooled, the diurnal average of operative temperature was 36.7°C. The diurnal average of operative temperature was reduced by 5.7°C if all the building fabrics were cooled. In this case, with pipes connected in series from the floor first to walls and then to roof resulted in 2.9°C lower operative temperature compared to that in the reverse sequence. Hence, the sequence in which the fabrics are cooled would have an appreciable influence on the performance of thermally activated building system.

Keywords

Passive cooling, Thermally activated building system, Cooling tower, Parametric analysis, Operative temperature, Thermal comfort

Accepted: 20 March 2017

Introduction

Thermally activated building system (TABS) has pipes embedded in building structures. Cold water is passed through these pipes to remove heat from the structure and in turn from the indoor space. The use of TABS was first reported in Switzerland during the 1930s. However, most of the earlier systems failed because of leakage and condensation problems.[1] In recent decades, these problems have been sorted out by adopting various strategies such as changing pipe material and controlling the supply water temperature.[2] Hence, the use of TABS has grown rapidly in recent years. Air conditioning requirements have also grown, due to urbanisation, change in lifestyle and heat island effects in cities.[3] However, the conventional mechanical cooling system is energy intensive and eco-destructive. Hence, energy-efficient TABS that can also provide better thermal comfort is the need of the hour.[4]

TABS can operate at a relatively higher water temperature, which increases the coefficient of performance (COP) of the chiller, and the indoor air temperature can be 1 or 2°C higher to achieve a thermal comfort level similar to that of the conventional air conditioner due

[1]Department of Mechanical Engineering, Indian Institute of Technology Madras, Chennai, India
[2]Department of Civil Engineering, Indian Institute of Technology Madras, Chennai, India

Corresponding author:
D. G. Leo Samuel, Indian Institute of Technology Madras, Refrigeration and Air Conditioning Laboratory, Chennai 600036, India.
Email: dglsam@gmail.com

to lower mean radiant temperature.[5] These make TABS energy efficient. In addition, the change in the working fluid from air to water and also the reduction in the quantity of air handled help reduce the energy consumption. Its ability to operate at relatively higher water temperatures allows it to be coupled with passive cooling systems like a geothermal system, cooling tower and nocturnal radiator.[6,7] This results in further energy saving. TABS also provides superior thermal comfort with noise and draft-free operation, a low vertical temperature gradient and direct treatment of the radiant load.[5,8]

TABS has been investigated extensively in the recent times.[9,10] Several of these investigations have focused on the energy-saving potential of the system. Meierhans[11] reported an annual energy saving of 6.5 MJ/m^2 for TABS supported with mechanical ventilation system compared to the conventional all-air system. Olesen[1] estimated 60 to 70% reduction in peak energy demand by TABS compared to the conventional cooling system. Zakula et al.[12] reported that TABS, with a dedicated outdoor unit, consumed 50% less energy compared to that by a variable air volume (VAV) system. A few studies on TABS have focused on thermal comfort and capital cost. A numerical study reported that in the packaged air conditioner (PAC), predicted percentage of dissatisfied (PPD) exceeded 10% limit for 30% of the time, whereas in TABS the limit is exceeded for only 2% of the time.[13] Olesen[1] reported that TABS reduces the initial cost of building due to the absence of separate cooling panels (used in the radiant panel system) and a smaller air supply duct. Another study reported that the cooling capacity of the chiller can be reduced by 50% due to the reduction in peak energy demand.[14] Sastry[15] did a case study on a symmetric building with a conventional cooling system in one of the symmetric parts and TABS in the another one. He reported that the cost of the conventional cooling system with all essential accessories, was ₹ 3327 per square metre, whereas that of TABS was marginally lower at ₹ 3302 per square metre.

Studies on coupling TABS with the passive cooling systems are scarce in literature. Pahud et al.[16] concluded that TABS is the most suitable cooling distribution system for geothermal cooling due to its best utilization of available cooling potential. Compared to a standalone PAC, a hybrid air-conditioning system with TABS, supported with a geothermal source to remove the sensible load and a PAC to remove the latent load, is reported to reduce the compressor energy consumption by 80 to 83% in residential buildings.[14] TABS supported with a cooling tower is reported to achieve thermal comfort in the hot and semi-arid summer climatic conditions of New Delhi, India, with indoor air temperature in the range of 23.5 to 28°C.[17] Very little research is focused on the influence of various parameters on the performance of TABS. Sattari and Farhanieh[18] investigated the influence of the number of pipes as well as their diameters and material in addition to the material and thickness of the floor cover on the performance of TABS for floor heating application. They concluded that the parameters related to piping have minimal influence on the performance of the system. Jin et al.[19] carried out a parametric study on TABS for floor cooling and concluded that water inlet velocity has minimal influence on floor temperature.

In all practical applications, it would be essential to control the cooling capacity of the system while in operation. However, in TABS, many parameters such as spacing, position, arrangement and diameter of pipe cannot be altered while operating the system. Hence, to control the cooling capacity, three parameters, namely inlet temperature and velocity of water and cooling surfaces (area), need to be controlled. The last of these can be controlled using valves and a proper water distribution system. In this paper, the influence of all the three parameters on the performance of a cooling tower-based TABS was investigated. Thermal comfort indices, namely, predicted mean vote (PMV), PPD and operative temperature (OT) were used in this study to quantify the performance of the system.

CFD simulation

Computational fluid dynamics (CFD) tools solve fluid flow problems using numerical techniques and algorithms. COMSOL Multiphysics, a commercially available CFD tool, was used to analyse the room depicted in Figure 1. The external dimensions of the room were assumed to be 3.46 m × 3.46 m × 3.15 m (equals the actual dimension of the experimentation room used for validation). Both the concrete roof and floor were 0.15 m thick, whereas all the four brick walls were 0.23 m thick. Cross-linked polyethylene (PEX) of inner diameter 0.013 m and wall thickness 0.0035 m was used in this study. The pipes were arranged in a serpentine layout with 0.2 m spacing between the adjacent pipes. They were positioned at the centre of both the roof and the floor. Ambient air was pushed into the room through a 3 m × 0.1 m opening located at the bottom of the south wall and the air escaped through a 0.8 m × 0.8 m opening located at the centre of the north wall. The room was ventilated at the rate of 4.2 air changes per hour (ACH). A uniformly distributed internal load of 15.6 W/m^3 was considered.

Parameters investigated

The parameters listed in Table 1 were varied to understand their influence on the cooling performance of

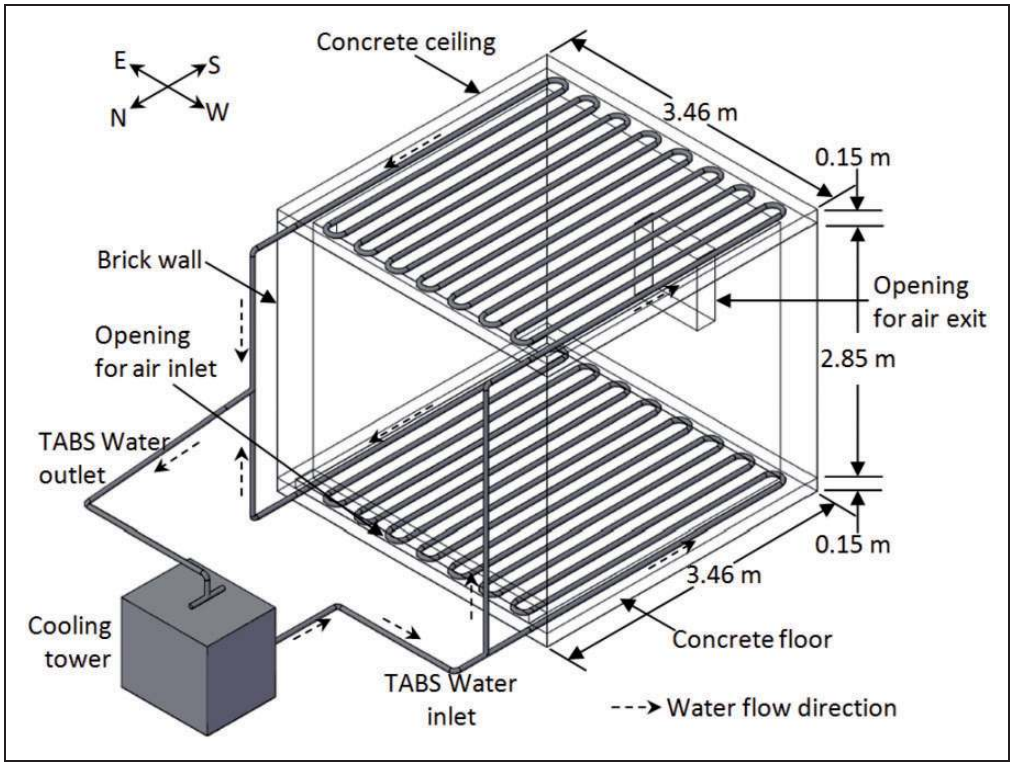

Figure 1. Schematic of a cooling tower-based TABS.

Table 1. Parameters investigated.

Sl. no.	Parameter, unit	Range	Increment	Default
1	Water inlet temperature, °C	WBT to WBT + 6	2	WBT
2	Water inlet velocity, m/s	0.2 to 1.0	0.2	0.4
3	Cooling surface (area)	R, RF, RF2W, AS	–	RF

WBT: wet bulb temperature; R: roof only; RF: roof and floor; RF2W: roof, floor and east and west walls; AS: all surfaces.

TABS and indoor thermal comfort of the room (Figure 1). The range, increment and default value of these parameters are also listed in the table. The range of these parameters was finalised based on practical feasibility. The parameters were varied one at a time in arithmetic sequence (incremental value present in the table), whereas the other parameters were maintained constant at their default value.

Governing equations

The Navier–Stokes equations, which apply Newton's viscosity law on the law of conservation of mass and momentum, and the Fourier law on the law of conservation of energy were used as the governing equations.[20] Equations (1) to (3) are the generalised governing equations that were applied for the complete model. These equations were simplified based on the nature of the domain. One such simplification was to change the governing equation to 1D for the cooling water in pipes due to its high length to diameter ratio.[21,22] The velocity of air at the ventilation inlet was very low. Hence, the air movement caused by natural convection would have an appreciable influence on the convective heat transfer.[23] This was accounted for by body force term (f) in the momentum equation (equation (2)).

$$\frac{\partial \rho}{\partial t} + \nabla \cdot (\rho u) = 0 \tag{1}$$

$$\rho\left[\frac{\partial u}{\partial t} + u.\nabla u\right] = -\nabla p + \nabla.\left(\mu\left(\nabla u + (\nabla u)^{T}\right) - \frac{2}{3}\mu(\nabla.u)I\right) + f \tag{2}$$

$$\rho C_p\left(\frac{\partial T}{\partial t}+u.\nabla T\right)=\nabla.(k\nabla T)+Q \tag{3}$$

where ρ is the density in kg/m^3, t is the time in seconds, u is the velocity in m/s, p is the pressure in Pa, μ is the dynamic viscosity in Ns/m^2, I is the identity matrix, f is the body force vector in N/m^3, C_p is the specific heat in J/kgK, T is the temperature in K, k is the thermal conductivity in W/mK and Q is the heat source in W/m^3.

Boundary conditions

The boundary conditions were specified by sol-air temperature and combined heat transfer coefficient. The sol-air temperature was calculated from the temperature of outdoor air and intensity of solar radiation. The former was obtained from the online metrological database,[24] whereas the latter was calculated with equations available in literature.[25] The influence of nocturnal long-wave radiation on the indoor thermal comfort parameters was very low and hence it was neglected. The temperature of water supplied to TABS was another important condition that needed to be specified. The water supplied to TABS was assumed to be at wet bulb temperature (WBT) at that instant, except for the parametric analysis of the water inlet temperature. WBT was calculated from the temperature and relative humidity of ambient air (equation (4)).[26]

$$\begin{aligned}T_w=&(T_a-273.15)\tan^{-1}\left[0.151977(RH+8.313659)^{0.5}\right]\\&+\tan^{-1}(T_a-273.15+RH)-\tan^{-1}(RH-1.676331)\\&+0.00391838(RH)^{0.75}\times\tan^{-1}(0.023101RH)+268.464\end{aligned} \tag{4}$$

where T_w is the WBT of ambient air in K; T_a is the dry bulb temperature of ambient air in K and RH is the relative humidity of ambient air in percentage.

Comfort indices

The thermophysical properties such as density, specific heat and viscosity of the building materials, air and water should be specified accurately. These properties, which depend on other variables such as the temperature and moisture content of the air, were specified accurately using equations available in literature.[27,28] Simulation results were processed to obtain the thermal comfort indices, namely, PMV, PPD and OT, which were then used to analyse the thermal comfort of the indoor space. PMV[29] and PPD[30] are the widely used thermal comfort indices for conditioned space. PMV represents the thermal comfort of a space with a thermal scale varying from –3 to +3 (–3 cold, –2 cool, –1 slightly cool, 0 neutral, 1 slightly warm, 2 warm and 3 hot). The PMV was calculated from six primary thermal comfort parameters, namely, indoor air temperature, mean radiant temperature (MRT), relative humidity and velocity of air, metabolism and clothing. PMV and PPD were calculated using equations (5) and (6), respectively. OT is another popular thermal comfort index, and this was calculated by averaging the indoor air temperature and MRT weighted by convective and radiative heat transfer coefficients (equation (7)).

$$\begin{aligned}PMV=&[0.303\times\exp(-0.036M)+0.028]\\&\times[M-W-E_d-E_s-L_R-D_R-R-C]\end{aligned} \tag{5}$$

$$\begin{aligned}PPD=&100-95\\&\times\exp\left[-\left(0.03353PMV^4+0.2179PMV^2\right)\right]\end{aligned} \tag{6}$$

$$T_0=(h_rT_{mrt}+h_cT_a)/(h_r+h_c) \tag{7}$$

where M is the metabolism rate in W/m^2, W is the external work in W/m^2, E_d is the evaporative heat loss by water vapour diffusion through skin in W/m^2, E_s is the evaporative heat loss by sweating in W/m^2, L_R is the latent heat loss by respiration in W/m^2, D_R is the sensible heat loss by respiration in W/m^2, R is the radiative heat loss in W/m^2, C is the convective heat loss in W/m^2, PPD is the predicted percentage of dissatisfied in percentage, T_o is the operative temperature in K, h_c and h_r are the convective and radiative heat transfer coefficients in W/m^{2}K, T_a is the temperature of indoor air in K and T_{mrt} is the mean radiant temperature of the indoor space in K.

Validation and mesh independence

Numerical studies are faster and cheaper compared to experimental work. However, results obtained from the former are not reliable unless validated by the latter. Our CFD simulation was validated with experimental data collected from a room with TABS constructed inside the premises of Indian Institute of Technology Madras, Chennai, India (Figure 2(a)). The room was modelled using a CFD tool (Figure 2(b)). The temperatures measured in the room external surfaces were used to specify the boundary conditions (Figure 3(a)). In addition, solar radiation data measured at the experimental site were used to specify the fenestration through glass windows and doors. In the experiment, the internal load was concentrated in the north-east corner of the room. Hence, the internal load was modelled to be uniformly distributed in a 0.6 m × 0.6 m × 1 m volume at the north-east corner. OT was calculated from the indoor air temperature

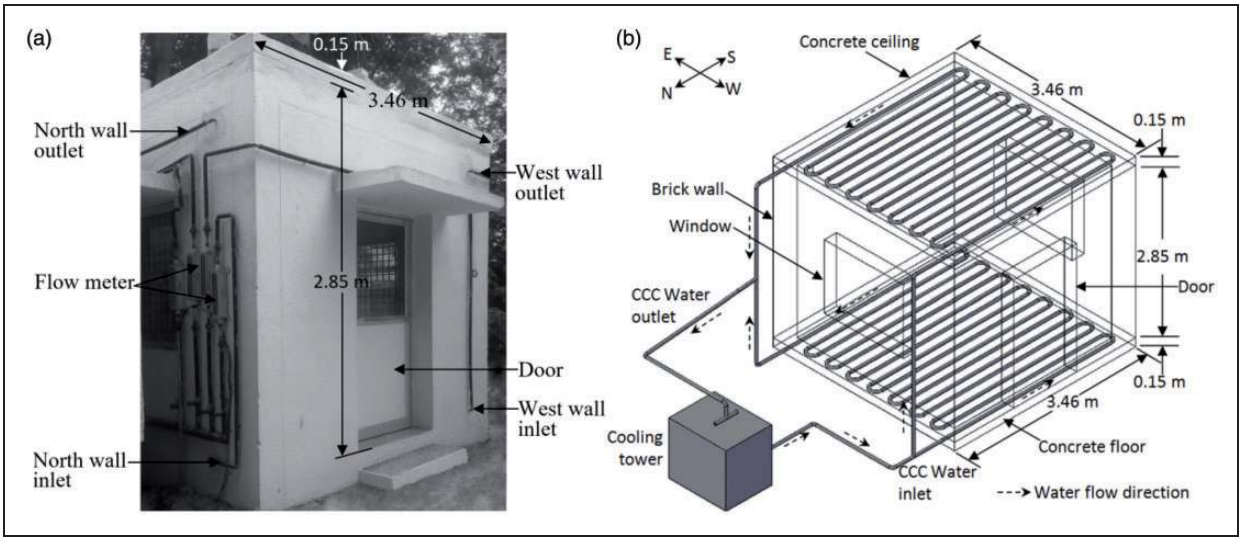

Figure 2. Validation: (a) experimental room and (b) CFD model.

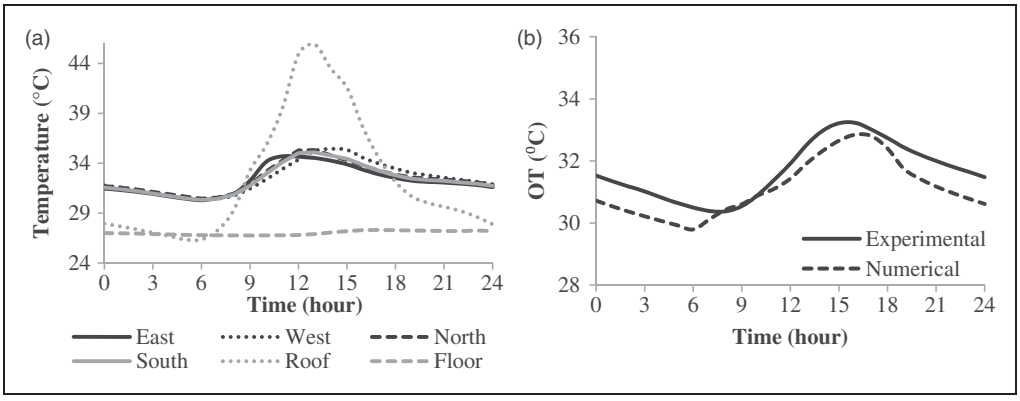

Figure 3. Validation: (a) boundary conditions and (b) comparison between experimental data and numerical output.

and MRT predicted by the model, and was found to agree well with the experimental data with a maximum deviation of 2.7% (Figure 3(b)). The detailed information about model geometry, simulation techniques, validation and mesh independent study are provided in an earlier paper published by the same authors.[9]

The model used for simulation (Figure 1) was simplified slightly with reference to the validation model (Figure 2(b)). In the experimental work, the monitoring equipment and the computer used to record data were placed together due to physical constraints, and these formed a major part of the internal heat load. However, in practical applications, the internal heat load could be distributed inside the room. Hence, in the model used for parametric analysis, the internal heat load was assumed to be uniformly distributed in the indoor volume. Large doors and windows are preferred in the humid climate of Chennai, where the experiments were conducted. However, in the hot and semi-arid climatic conditions of New Delhi, small doors and windows made of opaque materials such as wood are preferred. This reduces the heat transfer through the doors and windows. In addition, the influence of building openings on indoor conditions would be almost the same for different parametric values. Hence, the difference in comfort indices of indoor space between various parametric values would not be influenced significantly by assuming that the door and windows are absent in the building. However, this assumption would reduce the computation time dramatically.

Results and discussion

The quantitative influence of temperature and velocity of water at the inlet, and cooling surface (area) on thermal comfort parameters, namely, temperature and velocity of the indoor air, MRT, OT, PMV and PPD is discussed in this section.

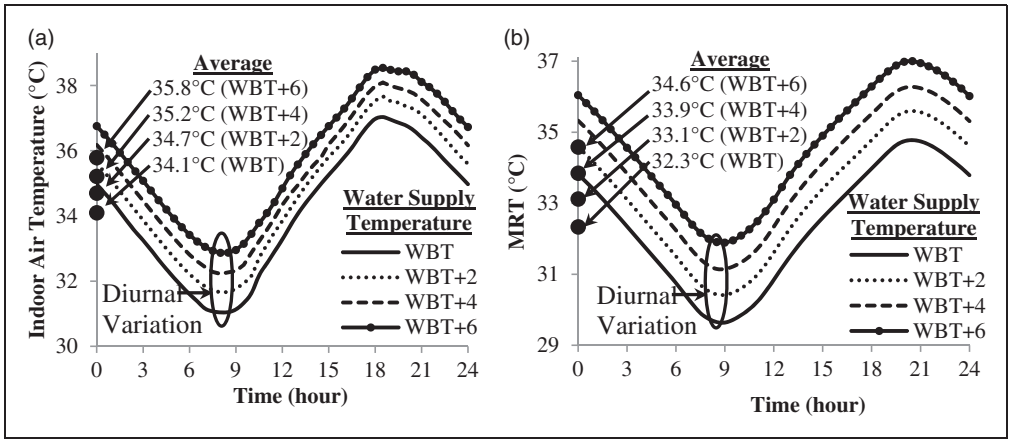

Figure 4. Influence of water inlet temperature on diurnal variation and average of (a) indoor air temperature and (b) MRT.

Water inlet temperature

Water inlet temperature was varied from WBT to WBT + 6°C with increments of 2°C to study its influence on the cooling performance of TABS. The increase in temperature of the cooling water at the inlet of TABS would reduce its heat removal potential and thus decrease the rate of heat removal. The heat removed by the water circulating through the pipes in the roof and floor declined by 451 and 187 W, respectively, when the inlet temperature of the water was increased from WBT to WBT + 6°C. This would result in a higher temperature of the room inner surfaces, for the higher water temperatures. Over the study range (WBT to WBT + 6°C), the average temperature of the inner surface of roof and floor was increased by 2.4 and 4.4°C, respectively. The change in heat removal rate was lower on the floor than on the roof, but the temperature change in the inner surface of the former was higher compared to that in the latter. This is because the bottom surface of the floor was considered to be insulated, and the convective heat transfer coefficient of its inner (top) surface was lower due to the relatively lower air movement in its vicinity. Hence, a higher temperature change of its inner surface would be essential even for a small change in the heat removal rate.

Figure 4 represents the influence of water inlet temperature on diurnal variation and average (marked on the vertical axis) indoor air temperature and MRT. The diurnal temperature trends of the indoor air were similar for different water inlet temperatures. The temperature of the indoor air was reduced during the early morning hours due to the drop in temperature of the outdoor air. The temperature reached the minimum at 8:00. After this, the indoor temperature was increased due to heating of the building by solar radiation and supply of unconditioned ventilation air that is at outdoor temperature. The temperature of indoor air reached the maximum at 18:30. Thereafter, it declined and reached the minimum the following day. The minimum and maximum temperatures of indoor air lagged behind that of outdoor air by 3 and 2½ h, respectively. This is attributed to the thermal inertia of the building. The increase in water inlet temperature from WBT to WBT + 6°C led to an increase in the temperature of indoor air by 1.7°C and MRT by 2.3°C. This is because the higher temperature water removed a lower quantity of heat. Within the study range, the indoor air temperature and MRT vary linearly for the change in water inlet temperature. For every 2°C increase in water inlet temperature, the temperature of indoor air increased by 0.6°C, whereas the MRT increased by 0.8°C. Water inlet temperature had no significant influence on the magnitude of diurnal fluctuation of both indoor air temperature and MRT and the times at which their extrema were reached.

Figure 5 compares the magnitude (background colour) and direction (red arrow) of indoor air movement on a vertical plane facing north for water inlet temperature of WBT and WBT + 6°C. The cold roof would cool the air in its vicinity. This cold air would drop down due to its higher density by replacing the warm air, while the hot air would move up due to its low density and was cooled by the roof. The cold air near the floor would resist the air movement because of its higher density, resulting in a relatively lower air movement at this location. A decrease in water inlet temperature would reduce the roof temperature and the temperature of indoor air in its vicinity. This would increase the buoyancy force of cold air, which in turn would increase the indoor air movement. The average velocity of indoor air increased by 9.6% when the water inlet temperature decreased from WBT + 6°C to WBT.

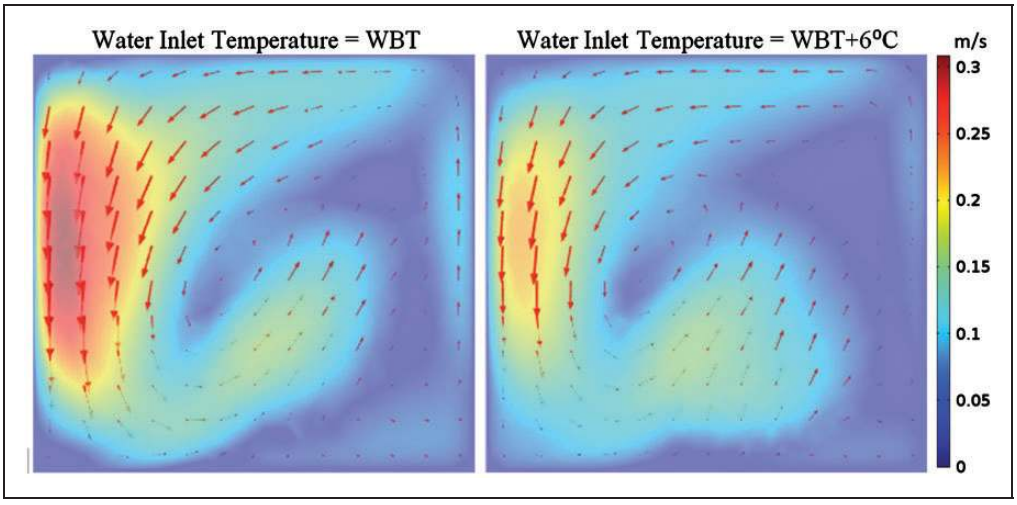

Figure 5. Indoor air velocity magnitude on a vertical north-facing plane at the centre of the room at 8:00.

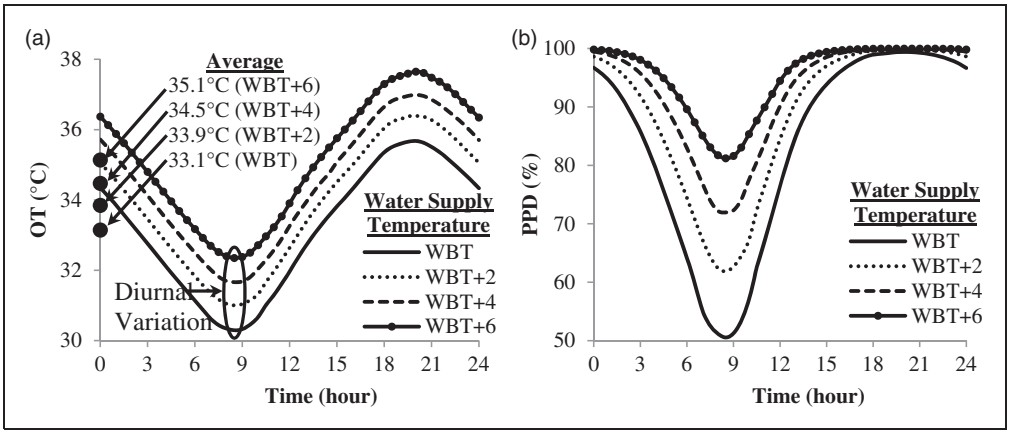

Figure 6. Influence of water inlet temperature on diurnal variation of (a) OT (b) PPD.

The increase in water inlet temperature increased the comfort indices (reducing the cooling performance), because of an increase in both the indoor air temperature and the MRT. Figure 6 represents the effect of the change in water inlet temperature on OT and PPD. Within the study range, the diurnal average of OT increased by 2°C. The diurnal average of the other two comfort parameters, namely PMV and PPD, increased by 0.6 and 11.9%, respectively, when the water inlet temperature increased from WBT to WBT + 6°C. Hence, a cooling tower with a lower approach should be preferred for a better cooling experience. Within the study range, both OT and PMV were observed to vary linearly with water inlet temperature. The supply water temperature was found to have no significant influence on the time at which the extrema of OT, PMV and PPD were reached and also on the amplitude of diurnal fluctuation of OT and PMV.

Water inlet velocity

For higher water inlet velocities (higher water flow rates), the temperature of the water would increase slowly along the flow compared to that of lower water inlet velocities (Figure 7). This is because more cooling water would be available in the former. Thus, for higher velocities, the cooling potential of water would drop slowly along the flow, which in turn would result in a higher rate of heat removal. For example, when the water inlet velocity was increased from 0.2 to 1 m/s, the diurnal average temperature of water at the exit of cooling pipes in the roof and floor decreased by 9.9 and 4.1°C, respectively, and the heat removed by the cooling water was enhanced by 563 and 83 W, respectively.

Figure 8(a) represents the change in the average temperature of the indoor air and inner surfaces of the building and the average velocity of the indoor air for

the change in water inlet velocity. The higher heat removal rate, for higher inlet velocities, would improve the cooling effect by reducing the temperature of indoor air and room inner surfaces, and comfort indices, but with a 'law of diminishing returns' trend. For example, the increase in water inlet velocity from 0.2 to 0.4 m/s decreased the temperature of roof inner surface by 1.7°C, whereas enhancing the velocity from 0.8 to 1 m/s reduced the temperature of the roof inner surface by 0.2°C only. Overall, increasing water inlet velocity from 0.2 to 1 m/s decreased the average temperature of the inner surfaces of the roof and floor by 3 and 1.7°C respectively. This, in turn, increased the convective heat transfer from the indoor air and reduced its diurnal average temperature by 1.3°C and the average temperature of the inner surfaces of the wall was reduced by 1.1°C. The temperature reduction in the wall for an increase in water inlet velocity was caused not only by the increase in the radiative heat transfer with cooler roof and floor but also by the enhancement of convective heat transfer with the cooler indoor air. A colder roof for the higher water inlet velocities would enhance the indoor air movement caused by natural convection. The increase in water inlet velocity from 0.2 to 1 m/s augmented the air velocity by 19%.

The increase in water inlet velocity would decrease the thermal comfort indices (i.e. enhances cooling), and thereby improve the thermal comfort of the indoor space. Figure 8(b) represents the diurnal variation and average (marked on the vertical axis) of OT for the different water inlet velocities. Increasing the water inlet velocity from 0.2 to 1 m/s decreased the diurnal average of OT from 34 to 32.6°C, but with a 'law of diminishing returns' trend. The diurnal average of OT reduced by 0.8°C when the water inlet velocity was increased from 0.2 to 0.4 m/s, but the reduction was just 0.1°C when the velocity was increased from 0.8 to 1 m/s. The other two thermal comfort indices, namely, PMV and PPD, were reduced by 0.4 and 11%, respectively, when the water inlet velocity was increased from 0.2 to 1 m/s. The inlet velocity of water had no significant influence on the amplitude of diurnal fluctuation of OT and PMV and also the time at which the extrema of the comfort indices were reached.

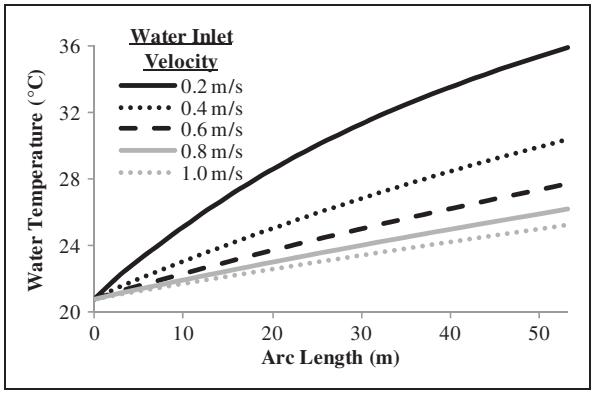

Figure 7. Water temperature inside the roof pipes at 12:00.

Cooling surface

The influence of increase in the number of cooling surfaces (areas) on the performance of TABS was studied by comparing four different scenarios listed in Table 2. For each scenario, three cases were studied. In Case 1, the cooling pipes to the various building fabrics (roof, walls and floor) were connected in series with the cooling tower, whereas in the remaining two cases, the connections were parallel. In Case 2, the water flow rate through the individual parallel loop was the same (191 l/h) for the

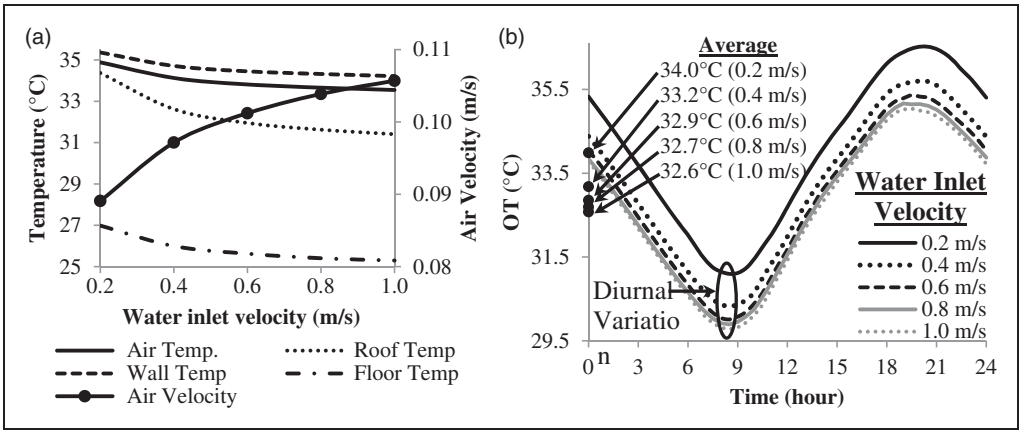

Figure 8. Influence of water inlet velocity on: (a) diurnal averages of temperatures and velocity and (b) diurnal fluctuation and average of OT.

Table 2. Scenarios investigated and the flow path for series flow configuration (Case 1).

S. no.	Name	Cooling scenario	Flow path for Case 1
1	R	Roof only	CT→R→CT
2	RF	Roof and floor	CT→F→R→CT
3	RF2W	Roof, floor and east and west walls	CT→F→E→W→R→CT
4	AS	All surfaces (roof, floor and all wall)	CT→F→N→S→E→W→R→CT

CT: cooling tower; F: floor; R: roof, E: east; W: west; N: north; S: south.

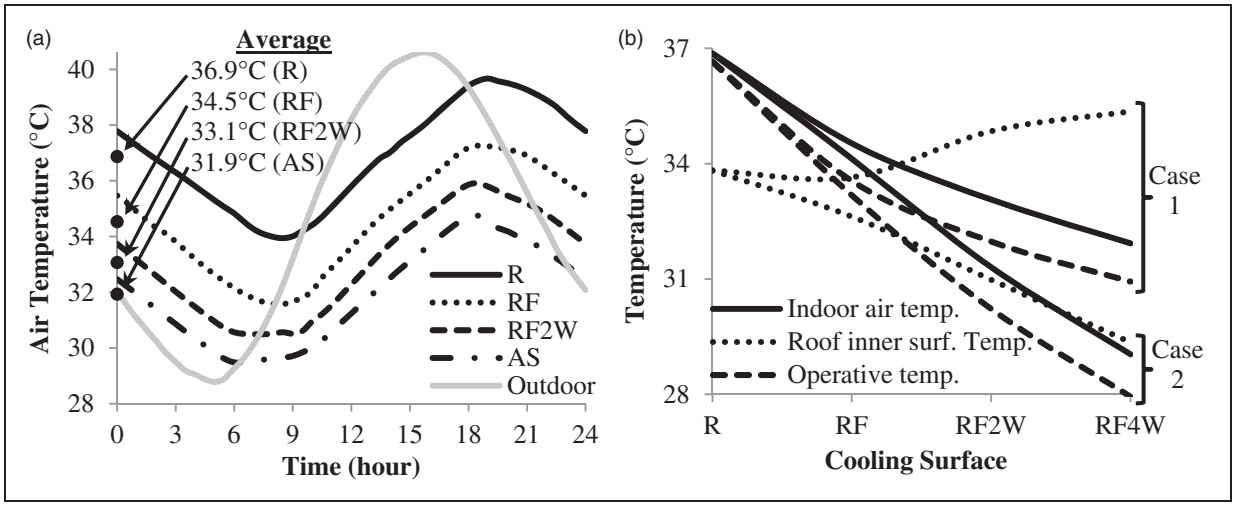

Figure 9. Influence of increase in cooling surface on (a) diurnal variation of OT and (b) average of thermal comfort parameters for Cases 1 and 2.

various scenarios, whereas in Case 3, the total water flow rate, i.e. the sum of water flow rate of parallel loops, was the same (0.191 m^3/h).

In Case 1, the flow of water through the cooling surfaces was sequenced in the ascending order of exposure to solar radiation (Table 2). For example, in all surfaces (AS) cooling, the water was first supplied to the floor, which would not receive solar radiation. The outlet water from the floor was supplied to the walls in the following sequence – north, south, east and west, and then to the roof, which would receive the maximum solar radiation. This sequence would provide maximum heat removal as the water first removed heat from the coldest building fabric, i.e. floor, and exited from the hottest surface, i.e. roof, which would have the maximum external heat load. The sequence in which the water flows was found to have an appreciable influence on the indoor comfort parameters. For AS cooling, the diurnal average of OT and PMV was 30.9°C and 1.7 if the water flow was in the above sequence (Table 2). When the flow of water was reversed, i.e. the water from cooling tower entered the roof and then flowed through the west, east, south and north walls in order and exited through the floor, the diurnal average of OT and PMV was increased (cooling performance decreases) by 2.9°C and 0.8, respectively.

An increase in the number of building fabrics that are cooled by TABS would enhance the heat transfer area, which would facilitate a higher rate of heat removal from the room. This would improve the cooling performance of the system. The average temperature of the indoor air was 36.9°C for R cooling. This was reduced to 34.5°C for RF cooling and further to 33.1 and 31.9°C for RF2W and AS cooling, respectively (Figure 9(a)). The pattern of diurnal variation was almost the same for the various cooling scenarios. However, with an increase in the number of cooling surfaces, the diurnal temperature fluctuation was decreased, as TABS would reduce the penetration of the highly fluctuating external heat. For R cooling, the diurnal temperature fluctuation of indoor air was 5.7°C. This was reduced by 0.5°C for AS cooling. An increase in the number of cooling surfaces would advance the times at which the extrema were reached. For R cooling, the minimum temperature of the indoor air was reached at 8:30, which advanced to 6:00 for AS cooling. This is attributed to the dissimilarity in the temperature difference between indoor and outdoor

air for the various scenarios. After sunset, the temperature of outdoor air would drop faster, while the temperature of indoor air would reduce slowly due to the thermal inertia of the building. This would result in a lower temperature of the outdoor air compared to that of the indoor air during the late evening and early morning hours. Hence, ventilation air would cool the indoor space during this period. For AS cooling, this period would end earlier due to the lower temperature of the indoor air as depicted in Figure 9(a). Hence, the ventilation air would start to heat the room earlier, compared to that of R cooling, so the minimum temperature would be reached earlier in AS cooling. The maximum temperature would also advance as TABS would remove the heat accumulated in the building fabrics during the day and would prevent the temperature increase during the evening hours.

Figure 9(b) depicts the influence of a change in the number of cooling surfaces on the average temperature of the indoor air and inner surface of the roof, and OT for Cases 1 and 2. In Case 1, the average temperature of the inner surface of the roof was increased with an increase in the cooling surface. This is because the cooling pipes were connected in series and the roof was the last building fabric in that series. Hence, the water supplied to the roof had already removed heat from all the remaining building fabrics that were present in the series connection. For example, in R cooling, the cooling water was supplied to the roof at WBT (average = 19.5°C), whereas in AS cooling, the water was supplied at a much higher temperature (average = 30.8°C), as it had already removed heat from the floor and all the four walls. Hence, the diurnal average temperature of the inner surface of the roof was 1.5°C higher for AS cooling compared to that of R cooling. This would reduce the velocity of indoor air with an increase in cooling surfaces, as the buoyancy force caused by cold air near the roof would reduce.

Excluding the inner surface of the roof, the temperature of the inner surface of the other building fabrics and indoor air would reduce with an increase in the cooling surfaces. This is because of the increase in the rate of heat removal, as the heat transfer area between the building fabrics and cooling water was increased with an increase in the cooling surface. The average temperature of the indoor air and inner surfaces of the floor and walls was 4.9, 11.6 and 5.8°C lower under AS cooling compared to that under R cooling. This reduced the indoor comfort indices (favourable). For AS cooling, the diurnal average of OT, PMV and PPD was 5.7°C, 1.7 and 38.3% lower compared to that of R cooling. The diurnal fluctuation of comfort indices was also reduced with an increase in the cooling surface due to a reduction in the temperature fluctuation of the indoor air and room inner surfaces. For R cooling, the diurnal fluctuations of OT and PMV were 5.3°C and 1.6. These were reduced to 4.7°C and 1.3, respectively, for AS cooling.

The influence of the cooling surface on the indoor comfort parameters was higher in Case 2 when compared to that of Case 1 (Figure 9(b)). This is because in Case 2, the cooling surface was increased along with a corresponding increment of the total water flow rate. Changing R to AS cooling reduced the OT by 8.7°C in Case 2, whereas in Case 1, the reduction was only 5.7°C. In Case 2, the average PMV and PPD were reduced by 1.7 and 38.3%, respectively, when R cooling was changed to AS cooling. Similar to Case 1, increasing the cooling surface advanced the extrema of the indoor comfort parameters. For example, in Case 2, the maximum OT for R cooling was reached at 20:00, which advanced to 18:30 under AS cooling.

The increase in the cooling surface had a lesser influence in Case 3 compared to that of Case 1. The diurnal average of OT for R cooling was 36.7°C. AS cooling reduced the diurnal average of OT by 5.7°C for Case 1, whereas the reduction was only 4.7°C for Case 3. The deviation in the cooling performance between these two cases was higher when more number of building fabrics were cooled, as depicted in Figure 10(a). The poor cooling performance of Case 3 compared to that of Case 1 was due to the ineffective usage of the cooling water in a less warm surface such as the floor. Figure 10(b) represents the diurnal variation of water temperature at the outlet of the roof and floor for RF cooling scenario of Cases 1 and 3, and the average of the roof and floor outlet temperatures for Case 3. In Case 1, the water was sent in through the floor inlet at WBT of ambient air and came out through the roof at an average temperature of 29.6°C. In Case 3, the water flow was divided into two equal parts and one part was sent to the floor, whereas the other was sent to the roof. The water which was sent through the floor removed lesser heat and came out at an average temperature of 24.8°C, whereas the average temperature of water at the exit of the roof was 33.1°C due to the relatively higher heat removal. The average of these two temperatures (29°C) was lower than the average temperature of water at the roof outlet in Case 1. Thus, the heat removal was lower in Case 3 compared to that in Case 1 and the cooling performance was poor in the former compared to that of the latter. In Case 3, an uneven distribution of water based on the cooling load of the building fabrics would improve the cooling performance of TABS. However, a sophisticated control system would be required as the cooling load would vary continuously due to the variation in the intensity of solar radiation and temperature of ambient air.

The diurnal fluctuation of OT was marginally lower in Case 1 compared to that in Case 3. For example, the

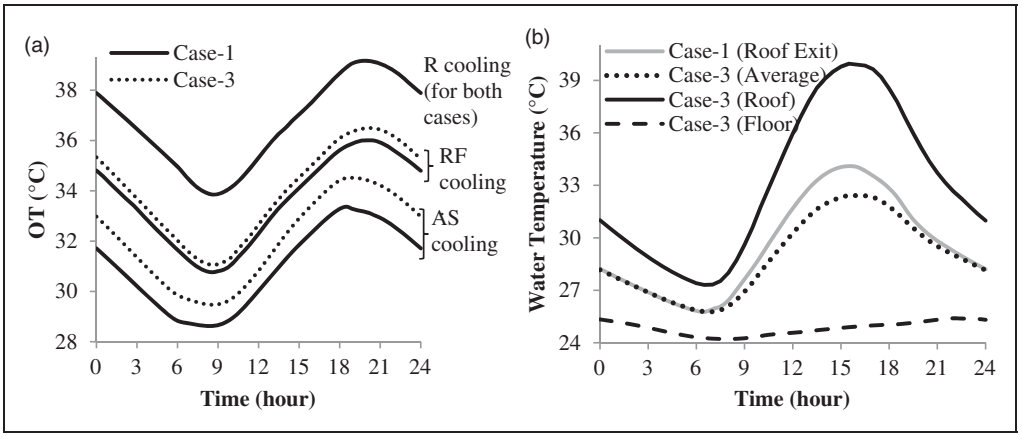

Figure 10. Diurnal variation of (a) OT for R, RF and AS cooling (b) water temperature at the exit for RF cooling scenarios of Cases 1 and 3.

Table 3. The best and worst cases of operating parameters.

Sl. no.	Parameter, unit	Worst	Best
1	Water inlet temperature, °C	WBT + 6	WBT
2	Water inlet velocity, m/s	0.2	1.0
3	Cooling surface (area)	R	AS

WBT: wet bulb temperature; AS: all surfaces.

OT was fluctuated by 4.7°C for the AS cooling scenario in Case 1, which was increased to 5°C in Case 3. The number of times at which the extrema were reached were the same in both cases.

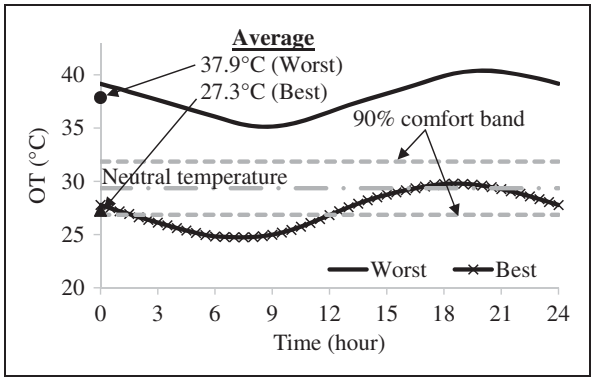

Figure 11. Diurnal variation and average of OT for the best and worst cases and adaptive comfort limits.

Combined influence

To understand the combined influence of these three parameters, the worst combination (Table 3) of these parameters is compared against that of the best. Figure 11 depicts the diurnal variation and average of the indoor OT along with the adaptive neutral temperature and 90% thermal comfort limits. The best combination of these parameters can improve the thermal comfort by reducing the PMV, PPD and OT by 3.1, 81% and 10.6°C, respectively, compared to that of the worst combination. The best combination also advances the extrema, which is attributed to a change in the cooling area from R to AS. The minimum and maximum OT for the worst combination was attained at 8:40 and 20:00, respectively, which advances by 1¼ and 1½ h, respectively, for the best combination. A marginal reduction in the diurnal fluctuation of the comfort indices was also observed for the best combination compared to the worst combination.

Considering the adaptive thermal comfort, the neutral temperature for the hot and semi-arid summer climatic conditions of New Delhi was calculated to be 29.4°C. For the worst case, the room was uncomfortably hot throughout the day with OT never fell below the 90% upper comfort limit. The best case that would improve the comfort and indoor space was within the adaptive comfort limits for most part of the day. During the morning hours, the room was over-cooled, which could be avoided by using a proper control system. The room that was modelled, resembled a standalone room such as a security guard room. All four walls and roof of the room were completely exposed to solar radiation. Hence, the room was shown to have a very high external heat load per unit area that is available for cooling with TABS. In addition, the internal heat load was considered to be in a higher range ($\approx 44\,W/m^2$). Even then, the proposed passive TABS supplied with water from the cooling tower was able to achieve the required thermal comfort. Hence, for a typical building, the proposed system could be used to achieve indoor thermal comfort as the external load per unit area of internal surfaces was relatively low due to self-shading of the building by its walls and roof,

Conclusions

The indoor thermal environment could be altered by changing the operating parameters. Thus, the present study quantified the influences of three operating parameters, namely, supply temperature and flow rate of water and cooling area of a TABS on the indoor thermal comfort. Within the study range, the temperature increase in the water supplied to TABS increased the indoor comfort indices (unfavourable) linearly, whereas the increase in flow rate and cooling surface decreased the comfort indices with a 'law of diminishing returns' trend. Among the three parameters investigated, cooling surface has the highest influence on the performance of TABS. For the climatic conditions of New Delhi, cooling all building fabrics would reduce the average operative temperature by 5.7°C compared to that of cooling of only the roof by TABS, when water is supplied at instantaneous wet bulb temperature with a flow rate of 191 l/h.

Authors' contribution

All authors contributed equally in the preparation of this manuscript.

Declaration of conflicting interests

The author(s) declared no potential conflicts of interest with respect to the research, authorship and/or publication of this article.

Funding

The author(s) disclose receipt of the following financial support for the research, authorship, and/or publication of this article: The authors thank the Department of Science and Technology, Government of India, New Delhi, for funding this study (Ref.: SR/S3/MERC/00091/2012).

References

1. Olesen BW. Using building mass to heat and cool. *ASHRAE J* 2012; 54: 44–52.
2. Meierhans RA. Slab cooling and earth coupling. *ASHRAE Trans* 1993; 99: 511–518.
3. Deneen MA, Gross AC and Mapes JL. Indoor climate control: the global demand for heating, ventilating, and air-conditioning equipment. *Bus Econ* 2010; 45: 126–134.
4. Rhee KN, Olesen BW and Kim KW. Ten questions about radiant heating and cooling systems. *Build Environ* 2017; 112: 367–381.
5. Tian Z and Love JA. A field study of occupant thermal comfort and thermal environments with radiant slab cooling. *Build Environ* 2008; 43: 1658–1670.
6. Helsen L. Geothermally activated building structures. In: Rees S (ed.) *Advances in ground-source heat pump systems*. 1st ed. Cambridge: Elsevier Science and Technology, 2016, pp.423–452.
7. Sprecher P and Tillenkamp F. Energy saving systems in building technology based on concrete-core-cooling. *Int J Ambient Energ* 2003; 24: 29–34.
8. Martínez FJR, Chicote MA, Penalver AV, Gonzalez AT and Gomez EV. Indoor air quality and thermal comfort evaluation in a Spanish modern low-energy office with thermally activated building systems. *Sci Technol Built Environ* 2015; 21: 1091–1099.
9. Rhee KN and Kim KW. A 50 year review of basic and applied research in radiant heating and cooling systems for the built environment. *Build Environ* 2015; 91: 166–190.
10. Romani J, Gracia A and Cabeza LF. Simulation and control of thermally activated building systems (TABS). *Energ Build* 2016; 127: 22–42.
11. Meierhans RA. Room air conditioning by means of overnight cooling of the concrete ceiling. *ASHRAE Trans* 1996; 102: 693–697.
12. Zakula T, Armstrong PR and Norford L. Advanced cooling technology with thermally activated building surfaces and model predictive control. *Energ Build* 2015; 86: 640–650.
13. Park SH, Chung WJ, Yeo MS and Kim KW. Evaluation of the thermal performance of a thermally activated building system (TABS) according to the thermal load in a residential building. *Energy Build* 2014; 73: 69–82.
14. Rijksen DO, Wisse CJ and van Schijndel AWM. Reducing peak requirements for cooling by using thermally activated building systems. *Energy Build* 2010; 42: 298–304.
15. Sastry G. First radiant cooled commercial building in India – critical analysis of energy, comfort and cost. In: *World energy engineering congress (WEEC) 2012*, Atlanta, October 30–November 2 2012; pp.1474–1479.
16. Pahud D, Belliardi M and Caputo P. Geocooling potential of borehole heat exchangers' systems applied to low energy office buildings. *Renew Energ* 2012; 45: 197–204.
17. Samuel DGL, Nagendra SMS and Maiya MP. Simulation of indoor comfort level in a building cooled by a cooling tower–concrete core cooling system under hot–semiarid climatic conditions. *Indoor Built Environ* (In print); Advance online publication; DOI: 10.1177/1420326X16635260.
18. Sattari S and Farhanieh B. A parametric study on radiant floor heating system performance. *Renew Energ* 2006; 31: 1617–1626.
19. Jin X, Zhang X, Luo Y and Cao R. Numerical simulation of radiant floor cooling system: the effects of thermal resistance of pipe and water velocity on the performance. *Build Environ* 2010; 45: 2545–2552.
20. Panton RL. *Incompressible flow*. 4th ed. New Jersey: John Wiley and Sons, 2012.
21. Barnard CL. A theory of fluid flow in compliant tubes. *J Biophys* 1996; 6: 717–724.
22. Lurie MV. *Modeling of oil product and gas pipeline transportation*. Weinheim: WILEY-VCH Verlag GmbH & Co., KGaA, 2008.
23. Incropera FP and Dewitt DP. *Fundamentals of heat and mass transfer*. 5th ed. New Delhi: Wiley-India, 2010.
24. Weather Underground. Weather history, www.wunderground.com (accessed 23 February 2015).
25. Sukhatme SP and Nayak JK. *Solar energy: principles of thermal collection and storage*. 3rd ed. New Delhi: Tata McGraw Hill Education Private Limited, 2008.
26. Stull R. Wet-Bulb temperature from relative humidity and air temperature. *J Appl Meteorol Climatol* 2011; 50: 2267–2269.
27. Tsilingiris PT. Thermophysical and transport properties of humid air at temperature range between 0 and 100°C. *Energ Convers Manage* 2008; 49: 1098–1110.
28. The Engineering ToolBox. Moist air properties, www.engineeringtoolbox.com (accessed 23 February 2015).
29. Fanger PO. *Thermal comfort analysis and applications in environmental engineering*. New York: McGraw-Hill, 1970.
30. Fanger PO. *Thermal comfort*. Malabar, FL: Robert E. Krieger, 1982.